Formation of Pt-based silicide contacts : kinetics, stochiometry and current drive capabilities

Guilhem Larrieu, Emmanuel Dubois, X. Wallart, Xavier Baie, J. Katcki

Formation of platinum-based silicide contacts: Kinetics, stoichiometry, and current drive capabilities

Cite as: Journal of Applied Physics **94**, 7801 (2003); https://doi.org/10.1063/1.1605817
Submitted: 16 April 2003 • Accepted: 08 July 2003 • Published Online: 02 December 2003

G. Larrieu, E. Dubois, X. Wallart, et al.

Formation of platinum-based silicide contacts: Kinetics, stoichiometry, and current drive capabilities

G. Larrieu, E. Dubois,[a] X. Wallart, and X. Baie
Institut d'Electronique de Microélectronique et de Nanotechnologie, IEMN/ISEN UMR CNRS 8520, Cité Scientifique, Avenue Poincaré, 59652 Villeneuve d'Ascq Cedex, France

J. Katcki
Institute of Electron Technology, Al. Lotników 32/46, 02-668 Warsaw, Poland

(Received 16 April 2003; accepted 8 July 2003)

A detailed analysis of the formation of Pt_2Si and PtSi silicides is proposed, based on x-ray photoelectron spectroscopy (XPS), transmission electron microscopy (TEM), and electrical characterizations. Published kinetics of the Pt_2Si and PtSi transformations under ultrahigh vacuum condition are consolidated on the basis of XPS measurements performed during an *in situ* annealing at a constant heating rate. At room temperature, an incomplete Pt_xSi reaction is clearly identified by XPS depth profiling. Using rapid thermal annealing at 300, 400, and 500 °C, the sequential Pt–Pt_2Si–PtSi reaction chain is found to be completed within 2 min. Outdiffusion of silicon to the top surface is shown to be responsible for the formation of a thin SiO_2 capping layer at 500 °C. Pileup of oxygen occurring at the Pt_2Si/Pt reaction front is clearly identified as an inhibiting factor of the silicidation mechanism. Another incomplete reaction scheme limited to the unique formation of Pt_2Si is exemplified in the case of ultra thin silicon-on-insulator films. Finally, current drive measurements on PtSi Schottky contacts have allowed us to identify 300 °C as the optimum annealing temperature while TEM cross sections demonstrate the formation of a smooth and continuous PtSi/Si interface at 300 °C. © *2003 American Institute of Physics.*
[DOI: 10.1063/1.1605817]

I. INTRODUCTION

Very thin films of metal silicides play an increasing important role in silicon integrated circuit technology as metal-oxide-semiconductor field-effect-transistors (MOSFETs) are shrunk below 0.1 μm of gate length.[1] Titanium, cobalt, and nickel silicides are commonly used in the semiconductor industry. The interesting properties of metal silicides, directly related to their utility in silicon technology, include thermal stability, low resistivity, and reduced silicide/silicon specific contact resistance. In order to further pursue down-scaling of MOSFETs in the 10–20 nm range of gate lengths, a significant effort must be devoted to the development of alternative architectures[2] that solves the many issues associated to the use of high κ dielectrics[3] and to the design of improved source/drain (S/D) regions. S/D are commonly based on a highly doped extension that provides the necessary configuration to obtain an excellent ohmic contact with a typical specific contact resistivity around $10^{-7}\,\Omega\,cm^2$. This last value is representative of the best midgap silicides.[4] A deeper insight in the challenges imposed to the S/D regions reveals tremendous constraints imposed to the dopant profiling and to the contact resistances. For instance, the lateral S/D doping steepness (1 nm/decade), the silicide thickness (5 nm), and the specific silicide/silicon contact resistance ($2.4 \times 10^{-8}\,\Omega\,cm^2$) are expected to reach very low targets in the perspective of a 10 nm physical gate MOSFET.[2] One possible solution to obtain a reduced specific contact resistance is to adopt a dual silicide approach according to which silicide materials with very low Schottky barriers to holes (ϕ_{bp}) and electrons (ϕ_{bn}) are integrated in *p*-type and *n*-type MOSFETs, respectively. Even more exciting, a MOSFET architecture using low Schottky barrier (ideally 0 eV) contacts has been recently proposed[5–7] in order to replace the conventional ohmic contacts on highly doped S/D. Pt and Ir based silicides (low ϕ_{bp}) and rare earth silicides like $ErSi_2$ (low ϕ_{bn}) are probably the best candidates for that purpose.[8,9] These perspectives reactivate a great deal of interest on platinum silicide. Much of the recent work on Pt_2Si and PtSi has focused on the kinetics and stoichiometry under ultrahigh vacuum (UHV) annealing conditions.[10–13] In this article, we propose a detailed study of the Pt silicidation mechanisms using various annealing conditions like UHV and rapid thermal annealing with a particular attention on the interface reaction at room temperature, on the influence of oxygen during silicidation reaction and on the optimum conditions to obtain the lowest specific contact resistance. After a description of the preparation techniques and measurement procedures in Sec. II, the kinetics and composition of Pt_2Si and PtSi silicides are critically analyzed using x-ray photoelectron spectroscopy (XPS) in Sec. III. Finally, Secs. IV and V provide electrical measurements and transmission electron microscopy (TEM) observations that consolidate the results of physical analysis.

[a]Author to whom correspondence should be addressed; electronic mail: emmanuel.dubois@isen.iemn.univ-lille1.fr

II. PREPARATION TECHNIQUES AND EXPERIMENTAL PROCEDURES

A. XPS analysis

The samples have been analyzed by XPS, using a Physical Electronics 5600 spectrometer fitted in an UHV chamber (base pressure 1×10^{-10} Torr). We use a monochromatized Al x-ray source ($h\nu=1487$ eV) and the detection angle is 45° with respect to the sample surface normal. For depth profile analysis, we use an Ar^+ ion gun with an ion energy of 1 keV and a beam raster of 5×5 mm^2. Concentration profiles are obtained using standard sensitivity factors provided by the manufacturer.[14] Sputter profiling induces the knock-on effect resulting in a smearing of the depth resolution. This is why, in order to minimize this effect, we have chosen a moderate ion energy of 1 keV. Under our experimental conditions, the induced broadening lies probably around 2 nm.[15] However, the following analysis of the XPS results (Sec. III) does not rely on thickness measurements from the depth profiles neither on a precise research of interface positions. Hence, the conclusions are not affected by this parasitic effect.

B. Sample preparation

Samples consist of pieces cut from (100) Si bulk or silicon-on-insulator (SOI) substrates (p type doped 4–10 Ω cm). A first degreasing step was performed in acetone followed by a rinse in isopropyl alcohol. A standard RCA cleaning step was subsequently applied to remove any possible surface contamination. Before being loaded into the vacuum deposition system, the surface oxide was removed by an HF:H_2O (1:100) dip for 30 s followed by a rinse in deionized water. Pt films were deposited by electron beam evaporation. The base vacuum before deposition was 2×10^{-8} Torr. A gentle surface etch was realized *in situ* using Ar sputtering at 60 eV during 20 s. Unless otherwise specified in the following of this paper, silicidation steps at various temperatures were processed by rapid thermal annealing (RTA) system (Jipelec).

C. Electrical measurements

The accurate determination of the barrier height of a silicide/silicon Schottky contact is a difficult task when this barrier is very low. A first reason is related to the silicon resistance connected in series with the Schottky contact. In the case of a weakly doped substrate, the silicon resistivity governs the current–voltage characteristic making the specific contact resistance hardly detectable. Another source of difficulty is the high level of reverse current flowing in through the Schottky junction that precludes an accurate discrimination between conduction and displacement currents when a capacitance–voltage method is considered.[16] Using internal photoemission measurements, the square root of photocurrent yield established by Fowler theory[17] becomes superlinear when applied to low Schottky barriers. In that specific case, the determination of the Schottky barrier height according to this method is therefore questionable. Another serious issue is related to the nature of the current transport

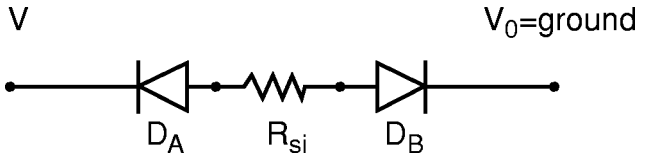

FIG. 1. Equivalent lumped circuit corresponding to two back-to-back Schottky diodes (D_A and D_B) separated by the silicon series resistance R_{si}.

mechanisms that involve a complex combination of the thermionic emission and field emission as outlined in the article by Crowell and Rideout.[18] A direct consequence is that the activation energy method in reverse mode can become less accurate because the slope of the $\ln(J_R/T^2)-1/T$ plot does not necessarily reflect the real barrier height.[19–21] In order to circumvent the aforementioned problems, an alternative method that characterizes the current drive capability of a Schottky contact has been set up. To reproduce the lateral configuration of the source/drain contacts of a MOSFET, measurements are performed between two Schottky contacts separated by a micrometer gap. This configuration also holds the advantage to eliminate any contribution of parasitic resistance associated with another type of metal–semiconductor interface (e.g., contact at the back side of the sample). The lumped equivalent circuit corresponds to two back-to-back Schottky junctions separated by the series resistance associated to the silicon gap as reproduced in Fig. 1. When an external voltage V is applied on a circuit terminal, one Schottky junction is forward biased while the second operates in reverse mode. Because a forward current increases exponentially with the applied voltage, this configuration ensures that the measured current is representative of the reverse biased junction providing that the silicon series resistance is negligible. Two criteria can be used to evaluate Pt-based silicides in terms of current performance. The first one is the maximum current drive when the contribution of the silicon series resistance is negligible compared to the Schottky contact resistance. In order to further justify the relevance of this parameter, Fig. 2 shows a typical Arrhenius plot for different voltages applied to the Schottky system depicted in Fig. 1. At a given applied bias (e.g., 0.5 V), two modes of operation can be distinguished. In the high temperature region, the silicon series resistance clearly governs the current, resulting in a pure ohmic behavior. In the low temperature region, the current is limited by the thermionic and field emission currents flowing over and through the Schottky barrier, respectively. The second criterion is the transition temperature between regimes governed by the silicon series resistance or by the Schottky contact resistance. Its determination is also illustrated in Fig. 2 at a given applied bias. For a same substrate type and doping, a low transition temperature reflects a low Schottky specific contact resistance and therefore a low value of the barrier height. In order to illustrate the relevance of this parameter, electrical simulations of the system formed by the two back-to-back Schottky junctions have been performed. The current–voltage model is taken from Crowell and Rideout's theory[18] extended to include the effect of image charge induction.[16] The voltage at each node of the lumped circuit given in Fig.

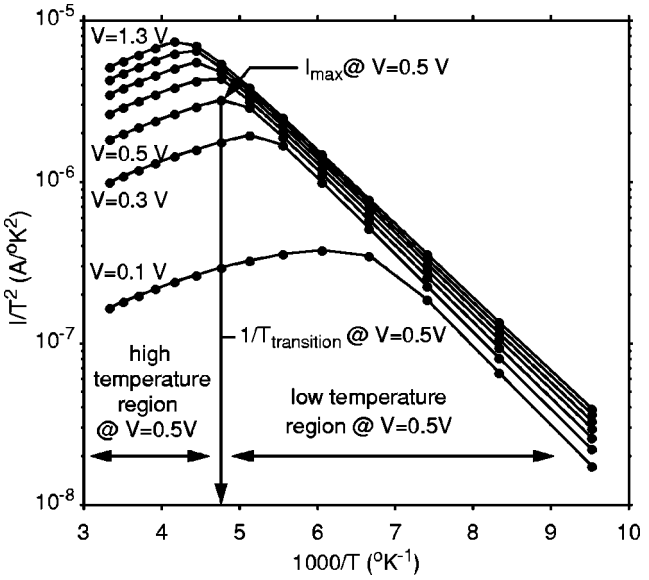

FIG. 2. Typical Arrhenius plot obtained for two back-to-back diodes on a weakly doped silicon substrate. The maximum current drive and the transition temperature are reported for a given value of the applied bias.

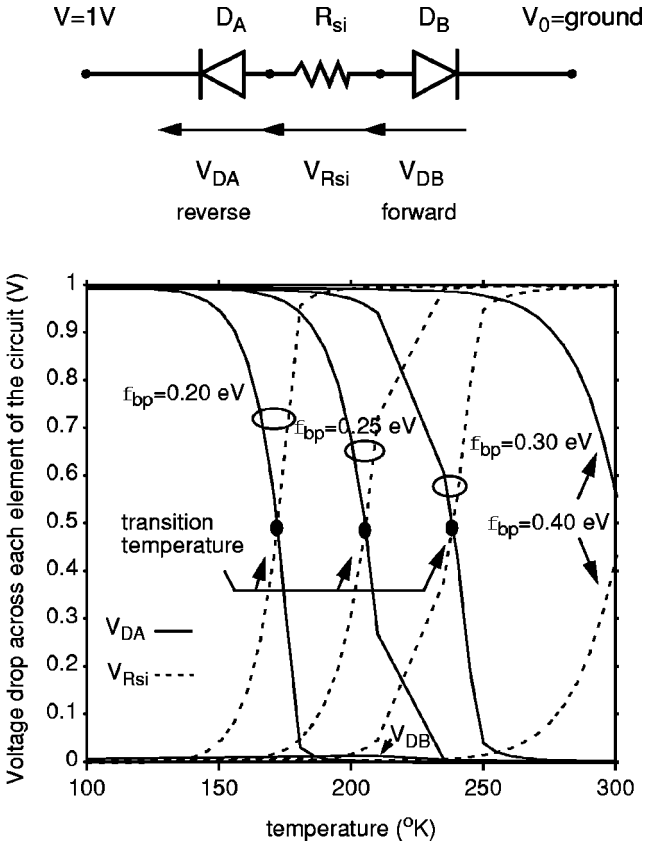

FIG. 3. Results of electrical simulation showing the voltage drop across each element of the equivalent lumped circuit formed by the two Schottky contacts and the silicon series resistance. The Schottky barrier height is taken as a parameter. A low transition temperature is relevant of a low Schottky barrier height.

1 is then determined by solving a nonlinear numerical system using a conventional Newton–Raphson procedure. Figure 3 represents the temperature dependence of the voltage drop across each element of the circuit for different values of the Schottky barrier height. For a low temperature, the total applied voltage matches the voltage drop across the reverse biased junction D_A indicating that the current flowing through the circuit is limited by this Schottky contact. As the temperature increases, the voltage drop across the silicon series resistance also increases up to a point corresponding to the transition temperature for which the external bias is equally distributed across D_A and R_{Si}. The careful inspection of Fig. 3 reveals that the transition temperature decreases when the Schottky barrier is reduced. As a conclusion, this parameter proves to be useful to classify Schottky contacts with respect to their barrier height and thus to estimate the quality of the silicide/silicon interface.

III. XPS ANALYSIS

A. Kinetics of platinum silicidation

Pt-Si intermixed layers can present three distinct types of composition PtSi, Pt_2Si, and Pt_3Si, but only the two first are stable forms.[22] Several studies have demonstrated that the platinum silicidation reaction is a two-step process governed by different energies of activation.[11,12] In the first reaction, Pt diffuses into Si to form an intermediate compound Pt_2Si, and

TABLE I. Typical activation energies related to Pt to Pt_2Si and Pt_2Si to PtSi reactions.

	Reaction (1): Pt_2Si formation Pt diffusion into Si				Reaction (2): PtSi formation Si diffusion into Pt_2Si			
	D_{Pt/Pt_2Si} $D=D_0\cdot\exp(-E_A/kT)$		Si consumption/Pt_2Si expansion		D_{Pt/Pt_2Si} $D=D_0\cdot\exp(-E_A/kT)$		Si consumption/PtSi expansion	
Reference	D_0 (cm²/s)	E_A (eV)	nm of Si per nm of Pt	nm of Pt_2Si per nm of Pt	D_0 (cm²/s)	E_A (eV)	nm of Si per nm of Pt	nm of PtSi per nm of Pt
[a]	—	1.3±0.2	0.66	1.43	—	1.5±0.2	1.32	1.97
[b]	—	1.55± 0.05			—	1.72± 0.05		
[c]	$3.7\times10^{1\pm1.55}$	1.50± 0.15			$2.7\times10^{1\pm1.95}$	1.70± 0.22		

[a]Reference 22.
[b]Reference 11.
[c]Reference 12.

in the second reaction Si diffuses into Pt_2Si to form a stable PtSi layer. These two reactions are known to occur sequentially: reaction (1) necessitates the complete consumption of the initial Pt layer before reaction (2), corresponding to the transformation of the Pt rich phase (Pt_2Si) into platinum monosilicide (PtSi),[22] starts. Both reactions are thermally activated. Table I summarizes typical measured values of the activation energy and of the pre-exponential diffusion coefficient in previously published experiments.[11,12,22] Accounting for the most recent data proposed by Stark *et al.*,[12] these activation energies are 1.50 ± 0.15 eV and 1.70 ± 0.22 eV, for the first and second reactions, respectively. In order to analyze the silicidation kinetics of each transformation, the same authors used Rutherford backscattering spectroscopy spectra analysis in conjunction with *in situ* ellipsometric measurements. Starting from a Pt overlayer of 23 nm and for an annealing step performed at a constant heating rate of 5 K/min, the conversion of Pt into Pt_2Si was found to be completed at 261 °C while the transformation of Pt_2Si into PtSi was obtained at 335 °C. Within the frame of this work, a similar type of annealing has been conducted into the XPS chamber under UHV condition. The initial Pt layer was 20 nm thick and the temperature was ramped from 20 to 550 °C in 120 min, corresponding to an average heating rate of 4.4 K/min. Only the top surface of the sample was analyzed by XPS during the annealing in order to detect the change of surface composition over 3λ, λ being the escape depth of 2.5 nm.[23] Figure 4(a) shows the temperature-dependent concentration corresponding to the $Pt\,4f$ and $Si\,2p$ emission lines. In order to accurately determine the characteristic temperature at which each transformation is completed, we have detected the most abrupt changes in chemical shift corresponding to the $Pt\,4f$ core level. Figure 4(b) shows a selection of $Pt\,4f$ spectra recorded during the annealing. As long as the annealing temperature is less than 245 °C, the position of $Pt\,4f_{7/2}$ peak is clearly centered at 71 eV, a binding energy relevant to elemental (metallic) Pt. The following spectrum recorded at 258 °C exhibits a sharp chemical shift of 1.5 eV that indicates that the Pt to Pt_2Si reaction front has reached the top surface. Spectra measured at temperatures up to 311 °C are also characterized by the same $Pt\,4f_{7/2}$ peak at 72.5 eV. At 324 °C, an additional 0.1 eV shift in the binding energy is clearly detected at 72.6 eV. Finally, from 338 °C to higher annealing temperatures, the $Pt\,4f_{7/2}$ peak remains centered at 72.7 eV indicating that the Pt_2Si intermediate phase has been fully converted into PtSi. In conclusion, reaction (1) (Pt_2Si formation by Pt diffusion into Si) and reaction (2) (PtSi formation by Si outdiffusion into Pt_2Si) are found to take place in the 245–258 °C and 324–338 °C intervals, respectively. Despite different heating rates and a thickness of the Pt overlayer that slightly differs, the temperatures related to the end of both silicidation reactions are found to be in excellent agreement with results published by Stark *et al.*[12] In order to get a more accurate determination of these characteristic temperatures, Fig. 5 represents the variations of the thickness of the formed Pt_2Si and PtSi silicide layers as a function of temperature, accounting for the two different

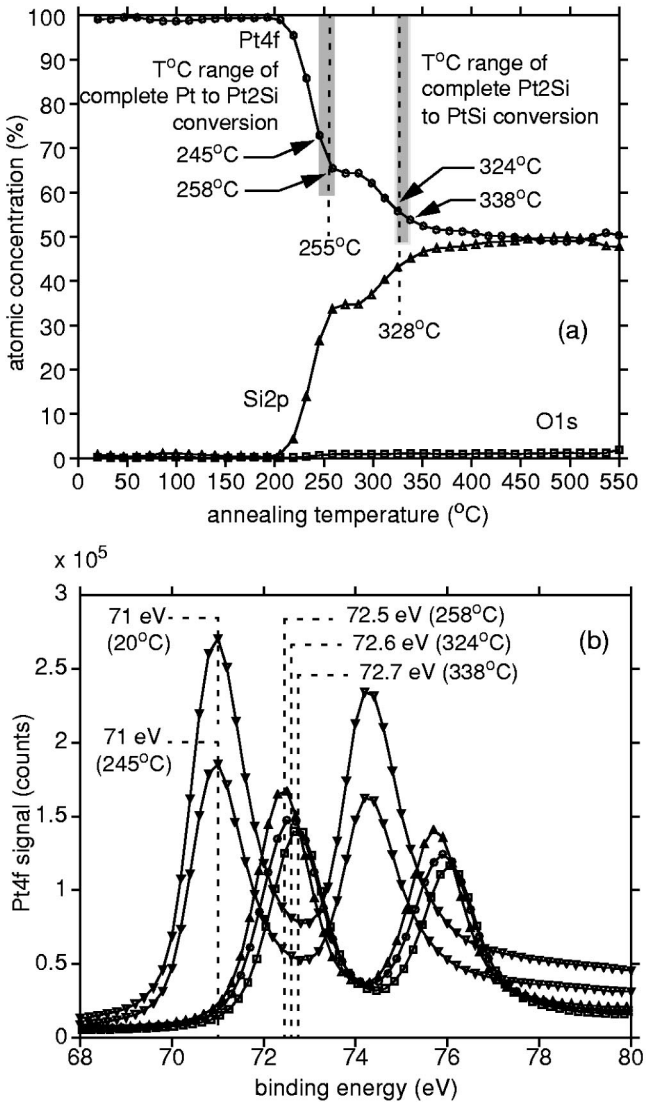

FIG. 4. Kinetics of silicidation reactions: (a) atomic concentration recorded by XPS during *in situ* annealing at a constant heating rate (4.4 K/min) under UHV condition. The temperature ranges at which the reaction fronts of the Pt_2Si and PtSi reactions reach the top surface are indicated. The most probable temperature of completion of each reaction (255 and 328 °C) is extracted from Fig. 5. (b) $Pt\,4f$ spectra recorded at some specific temperatures around the Pt_2Si and PtSi transitions.

heating rates, i.e., 5 K/min. in Ref. 12 and 4.4 K/min in this work. These curves have been obtained using a classical growth rate equation given by

$$d_x^2 = \int_0^t D_x dt = \int_{T_0}^{T_x} D_x (dT/dt)^{-1} dT$$

$$= D_{0x}(dT/dt)^{-1}\frac{k_B}{E_{Ax}}\left\{T_x^2 \exp\left(-\frac{E_{Ax}}{k_B T_x}\right) - T_0^2 \exp\left(-\frac{E_{Ax}}{k_B T_0}\right)\right\}, \quad (1)$$

where x stands for 1 or 2 for the first or the second reaction, respectively. T_x is the temperature at which each one of the above reactions is fully completed. E_{Ax} is the activation energy, D_x, the temperature-dependent diffusivity, and D_{0x} the

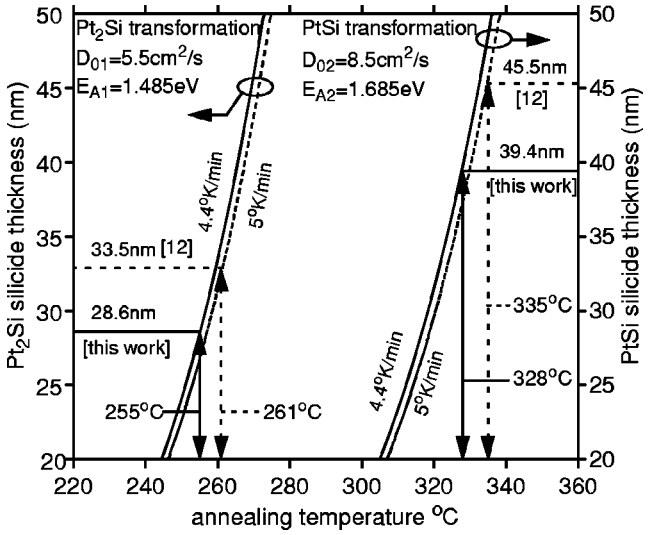

FIG. 5. Thickness of the Pt_2Si and PtSi phases accounting for different heating rates. The pre-exponential diffusion coefficients are fitted to match results published in Ref. 12 using an annealing ramp of 5 K/min. In the present experiment performed at 4.4 K/min, the temperatures of complete silicidation (255 and 328 °C for Pt_2Si and PtSi transformations, respectively), are extracted using $D_{01}=5.5\ \mathrm{cm^2/s}$, $D_{02}=8.5\ \mathrm{cm^2/s}$, $E_{A1}=1.485$ eV, and $E_{A2}=1.685$ eV.

pre-exponential diffusion coefficient. T_0 is the starting temperature set at 20 °C. Given the large error bars associated to results of previously published work[12] (e.g., the min–max values of D_{0x} vary over 3 decades), the following procedure has been used to better estimate the most probable characteristic temperatures of complete silicidation in the present experiment.

(i) Assuming that the average activation energies $\langle E_{A1}\rangle = 1.485$ eV and $\langle E_{A2}\rangle = 1.685$ eV are the most representative of the silicidation experiments conducted by Stark *et al.*,[12] the mean pre-exponential diffusion coefficients $\langle D_{01}\rangle$ and $\langle D_{02}\rangle$ must be set to 5.5 and 8.5 $\mathrm{cm^2/s}$ in order to match the final thickness of the Pt_2Si and PtSi phases, 33.5 and 45.3 nm reached at temperatures of 261 and 335 °C, respectively.

(ii) Considering that the above values of $\langle E_{A1}\rangle$, $\langle E_{A2}\rangle$, $\langle D_{01}\rangle$ and $\langle D_{02}\rangle$ also hold in the case of our experiment, the characteristic temperatures are found to be 255 and 338 °C (Fig. 5) to match the final thickness of the Pt_2Si and PtSi phases, established at 28.6 and 39.4 nm, respectively.

B. Platinum silicide at room temperature

It has been reported that Pt can react with silicon at room temperature resulting in the formation of an intermixed Pt–Si layer. Using high resolution cross-sectional TEM analysis, Donaton *et al.*[24] observed the formation of a continuous, smooth and uniform 3 nm thin PtSi layer obtained after Pt deposition and selective chemical etching, on top of which a thin layer of silicon oxide was formed. XPS experiments confirmed the same characteristics of silicide bonds before and after a subsequent rapid thermal annealing at 450 °C. One of their conclusions was that the sputtering technique used to deposit Pt provides sufficient energy to sputtered atoms to initialize the silicidation reaction. In contrast, other works also report the presence of Pt–Si bonds when Pt is evaporated on a clean silicon substrate kept at low temperature, i.e., without bringing any notable source of energy to activate the silicidation mechanism.[25] In order to investigate the initial interfacial reaction, a 15 nm thick Pt layer was evaporated following the procedure described in Sec. II B. It is worth noting that the sample was not heated during this deposition step. An XPS depth profile was recorded on that sample in order to detect a possible reaction between Pt and Si. The original photoemission measurements of the Pt $4f$ and Si $2p$ core levels have been fitted using a standard linear least squares procedure[14] to identify the chemical states of each element (Si and Pt) that appear in the depth profile. Figure 6(a) shows the resulting decomposition of the Pt $4f$ profile into two Pt $4f(\mathrm{Pt}_x\mathrm{Si})$ and Pt $4f$(Pt) contributions. The extracted basis of spectra used to calculate the two deconvolved depth profiles is given in Fig. 6(c). The Pt $4f$ spin–orbit doublet ($4f_{5/2}$,$4f_{7/2}$) exhibits a chemical shift of 1.5 eV from 71 to 72.5 eV that reveals the activation of a silicidation reaction involving the formation of a Pt_xSi-like layer.[10,26,27] This result is consolidated by Fig. 6(b) that gives the decomposition of the Si $2p$ profile into its two Si $2p(\mathrm{Pt}_x\mathrm{Si})$ and Si $2p$(Si) expected contributions. The corresponding basis of spectra is also shown in Fig. 6(d) revealing a chemical shift from 99.2 to 99.8 eV of the Si $2p$ emission line, which is again attributed to the presence of silicide-like bonds.[10,27] Figure 6(e) gives a summarized picture of the Si and Pt concentration depth profiles depending on the chemical environment of each element. It can be concluded that silicide is formed although it is not possible to determine the exact composition nor to conclude on the uniformity of the silicide layer. Nevertheless, the variations of the individual Si $2p(\mathrm{Pt}_x\mathrm{Si})$ and Pt $4f(\mathrm{Pt}_x\mathrm{Si})$ profiles over a period covering 30–80 min of sputtering time does not seem indicative of a stable stoichiometric composition. However, these profiles can be affected by the knock-on effect induced by the sputtering as suggested by the observed tail of the Pt signal at long sputtering time and hence do not allow us to go further in the analysis of the interfacial compound.

C. Platinum silicide formation at 200 °C

Because the silicidation reactions involving Pt are governed by a diffusion mechanism, a significant part of the initial Pt layer can react at a relatively low temperature. Zhou *et al.*[11] have found that the two major reactions (formation of Pt_2Si and PtSi) are preceded by an initial transformation taking place between 100 and 200 °C and characterized by a very low activation energy of 0.19 ± 0.043 eV. In the present contribution, we have investigated the silicidation reaction obtained by RTA at 200 °C for 2 min, starting from an initial Pt layer of 15 nm. Figure 7 gives the corresponding atomic concentration depth profile obtained by XPS analysis. Over the range of 30–50 min of sputtering time, the concentrations of Pt and Si clearly outline a zone of reaction over which a partial transformation of Pt into Pt_xSi ($x\sim2$) takes place. More surprisingly, we find a significant presence of

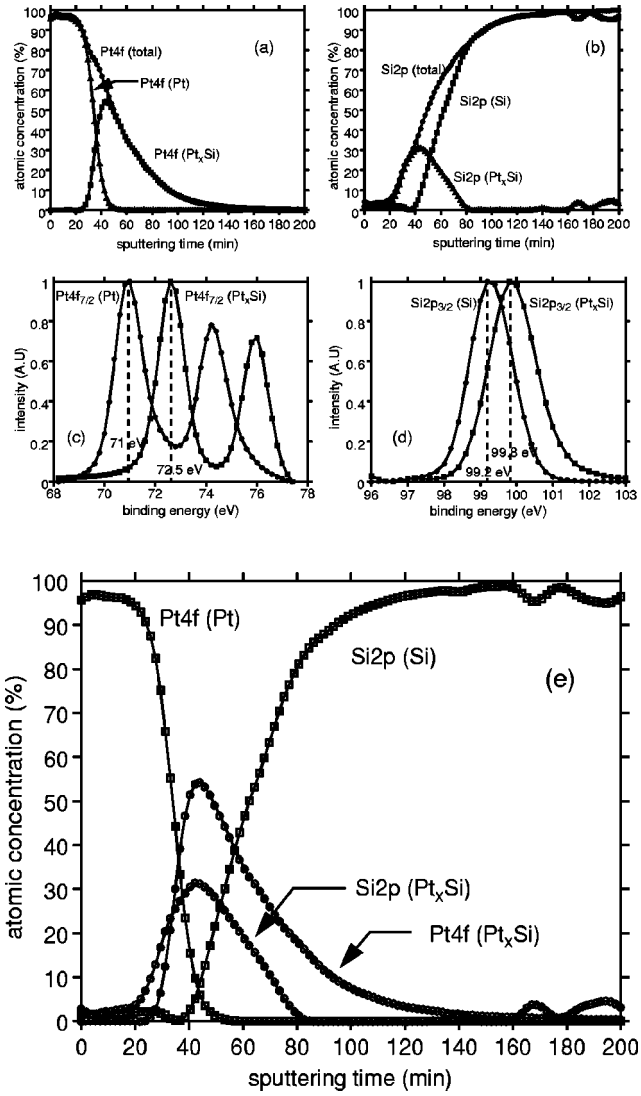

FIG. 6. XPS analysis of the initial Pt–silicide reaction occurring at room temperature: (a) Pt $4f$ depth profile deconvolved into its Pt $4f$(Pt_xSi) and Pt $4f$(Pt) contributions; (b) Si $2p$ depth profile deconvolved into its Si $2p$(Pt_xSi) and Si $2p$(Si) contributions; (c) extracted basis of spectra used in the deconvolution of the Pt $4f$ profile shown in (a): 71 and 72.5 eV are relevant of metallic and silicide-like binding energies; (d) extracted basis of spectra used in the deconvolution of the Si $2p$ profile shown in (b): 99.2 and 99.8 eV are relevant of elemental silicon and Pt_xSi-like binding energies; and (e) summary of atomic concentration depth profiles obtained from Pt $4f$ and Si $2p$ photoemitted electrons according to their chemical environment.

silicon close to the initial surface between 10 and 20 min of sputtering time, indicating that the reaction front is probably not as sharp and uniform as assumed for ellipsometric measurements.[12] In this region, the Si $2p_{3/2}$ photoemission line is essentially centered at a binding energy of 100 eV attributed to silicide-like bonds.

D. Platinum silicide formation above 300 °C

As outlined previously, Pt reacts first with Si to form Pt_2Si and only after all Pt has been consumed in this way, the second reaction of Pt_2Si to PtSi starts. For annealing temperatures above 300 °C, the diffusivities D_1 and D_2 of the two sequential Pt to Pt_2Si and Pt_2Si to Pt silicidation mechanisms are large enough to ensure that both reactions are fully

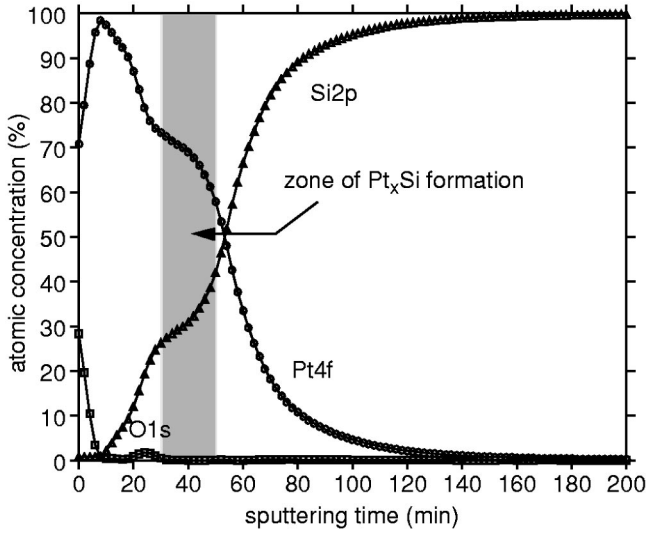

FIG. 7. XPS atomic concentration depth profile obtained from a sample annealed by RTA at 200 °C for 2 min. The shaded zone corresponds to a reacted Pt_2Si phase covered by metallic Pt.

completed when a sufficiently thin layer of Pt is considered. Starting from an initial Pt layer of 15 nm, the Pt_2Si reaction takes less than 3 s at 300 °C while the full silicidation into PtSi requires less than 120 s. These times of reaction have been obtained using the conventional square-root dependence of the silicide thickness with time described by Eq. (1). Their calculation accounts for the average diffusion parameters determined with the help of Fig. 5 and based on the results of Stark *et al.*[12] From the above analysis, the PtSi silicidation mechanism is expected to be fully completed within the 2 min of annealing performed at 300, 400, and 500 °C starting from the same 15 nm thick Pt overlayer. XPS depth profiles have been recorded for these three annealing conditions and are presented in Figs. 8, 9, and 10, respectively. Stoichiometric PtSi is obtained sufficiently far from

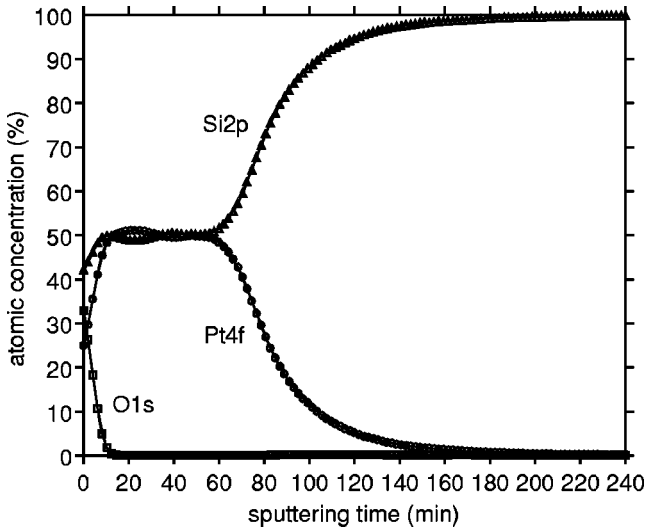

FIG. 8. XPS atomic concentration depth profile obtained from a sample annealed by RTA at 300 °C for 2 min. The PtSi silicidation reaction is fully completed as shown by the stochiometric Pt and Si concentrations. The Pt overlayer is 15 nm.

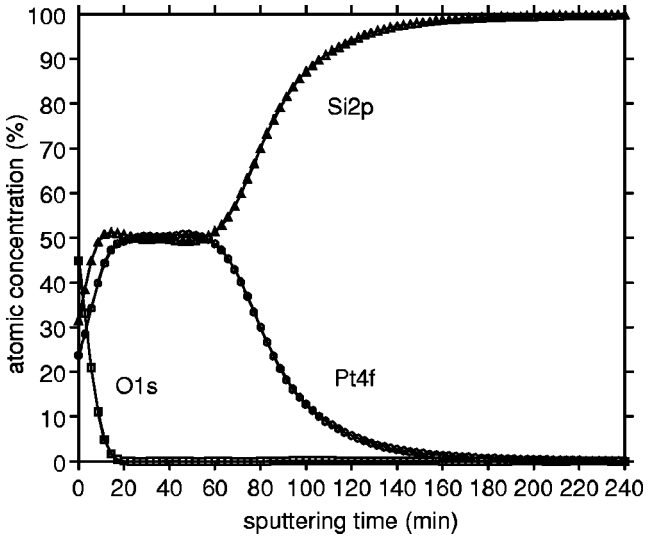

FIG. 9. XPS atomic concentration depth profile obtained from a sample annealed by RTA at 400 °C for 2 min. The Pt overlayer is 15 nm.

the top surface. For the three annealing conditions and at a typical sputtering time of 50 min relevant to platinum monosilicide, the Pt $4f_{7/2}$ emission line is centered at 72.7 eV resulting in a chemical shift of 1.7 eV[26,27] with respect to metallic Pt (71 eV). Consistently, the Si $2p$ emission peak is displaced from the 99.2 eV emission position of clean p-Si(100) to 100.1 eV relevant of PtSi formation. One important feature that can be observed when the annealing temperature reaches 500 °C (Fig. 10) is the significant increase of oxygen concentration present at the top surface. This effect is attributed to silicon outdiffusion, the diffusion species during PtSi formation. From a quantitative viewpoint, the ratio between the surface atomic concentrations of oxygen and silicon is close to 2:1 indicating that the top layer could be composed of silicon dioxide. At the beginning of the sputtering phase, a careful inspection of Fig. 10(c) reveals that the dominant peak of the Si $2p$ emission line is centered around 103.8 eV, while a secondary peak is centered at 100.1 eV. The first binding energy is consistent with the presence of SiO_2,[28,29] whereas the second peak is typical of PtSi-like bonds. As the sputtering process proceeds, the Si $2p$ peak at 103.8 eV vanishes while the 101.1 eV emission line clearly increases as the PtSi layer is uncovered during depth profiling. Considering now the O $1s$ photoemission spectra of Fig. 10(b), it can be observed that the initial peak position located at 533.1 eV[29,30] slightly moves to a lower binding energy of 532.4 eV before disappearing when sputtering reaches the PtSi layer. The above range of O $1s$ peak positions are also characteristic of the presence of the SiO_2 and consolidate the interpretation based on the analysis of the Si $2p$ spectra.

E. Incomplete silicidation reaction due to oxygen pileup

Crider and co-workers[22] established that the growth rates and phase growth sequence of Pt_2Si and PtSi silicides were not affected by chemical etching with fluoridric acid, by sputter cleaning with Ar or by the presence of nitrogen under a partial pressure of 10^{-7} Torr during the Pt deposition step.

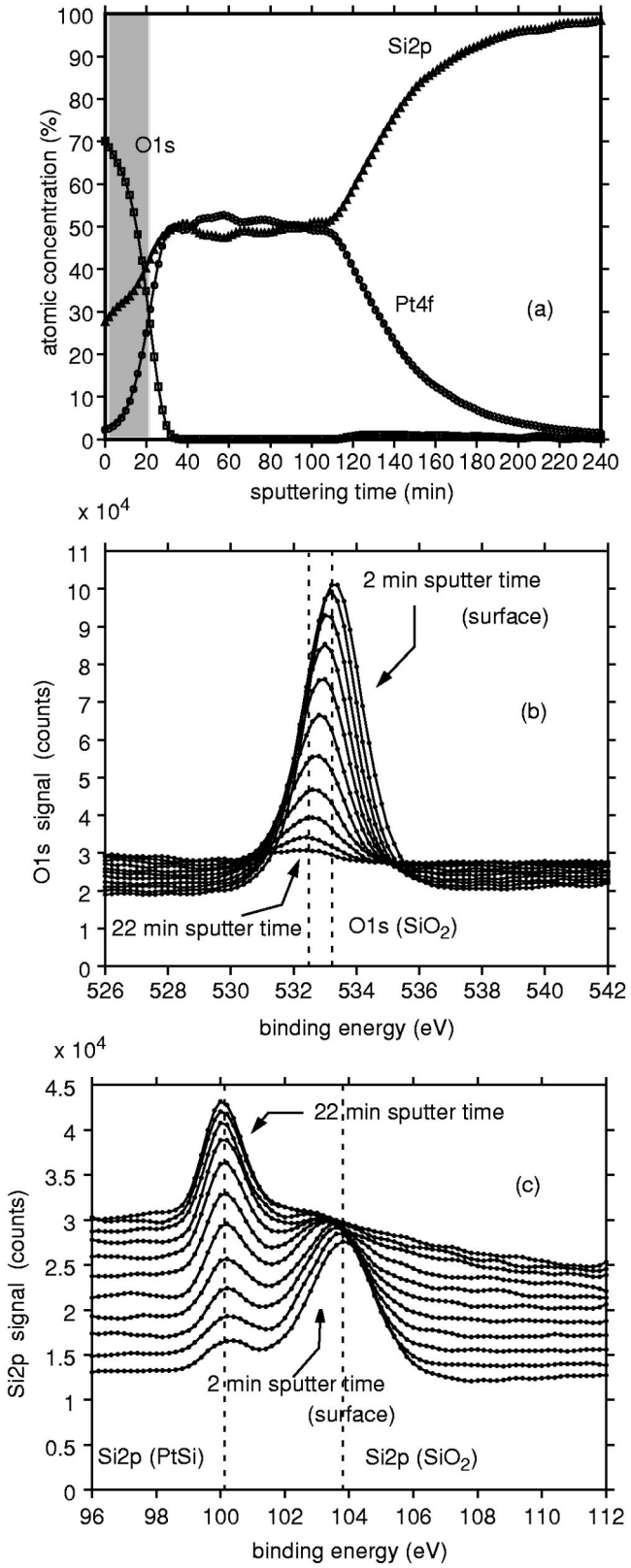

FIG. 10. XPS analysis of a sample annealed by RTA at 500 °C for 2 min starting from a 15 nm Pt overlayer: (a) atomic concentration depth profile showing stochiometric PtSi covered by SiO_2 formed by Si outdiffusion and oxidation; (b) series of O $1s$ spectra recorded close to the surface: the O $1s$ peak centered in the 532.4–533.1 range indicates the presence of SiO_2; (c) series of Si $2p$ spectra recorded in the shaded zone of (a): the Si $2p$ peak centered at 103.8 eV (top surface SiO_2) vanishes rapidly while the second peak centered at 100.1 eV dominates when the stochiometric PtSi phase is reached.

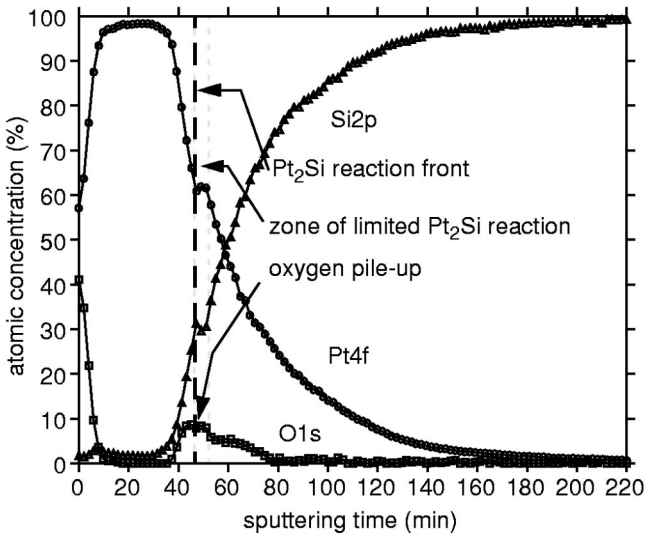

FIG. 11. XPS atomic concentration depth profile of a sample annealed at 300 °C during 30 min in a conventional tubular oven under N_2 flow but exposed to ambient oxygen during the introduction phase. The diffusion of O_2 into Pt stops the Pt_2Si reaction front.

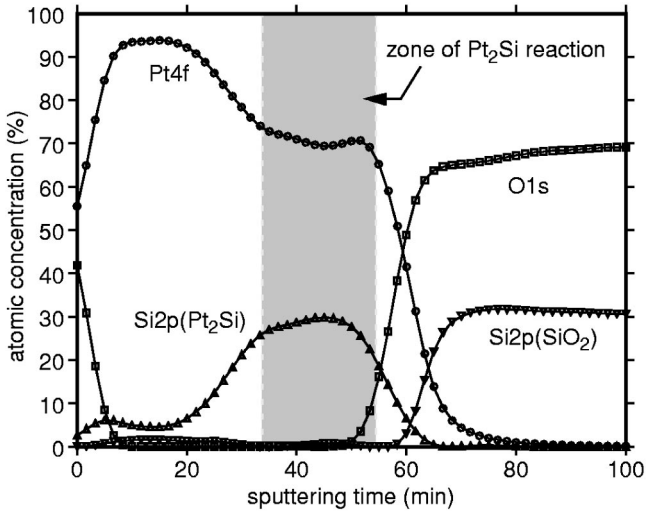

FIG. 12. Silicidation of a thin (8 nm) SOI film: XPS atomic concentration depth profile after annealing by RTA at 300 °C for 2 min. The Pt_2Si reaction is stopped after the complete consumption of silicon (SOI) layer.

In contrast, a significant decrease in both Pt_2Si and PtSi diffusivities was observed when the Pt film was evaporated under 10^{-8} Torr of oxygen partial pressure. In this last case, the simultaneous existence of Pt, Pt_2Si, and PtSi can be observed because oxygen is known to pile up at the advancing Pt_2Si front.[22] Within the frame of this study, a 15 nm thick layer was deposited under the same cleaning and evaporation conditions than previous samples for which no abnormal silicidation reaction is observed. The annealing was performed in a conventional tubular oven at a temperature of 300 °C under a continuous flow of nitrogen. Because the introduction of the sample is made under ambient atmosphere, a significant amount of oxygen is present in the heating pipe at the beginning of the silicidation reaction. Figure 11 shows the resulting XPS depth profile obtained after a 30 min annealing step. A significant concentration of oxygen is observed within the top Pt film with a clear accumulation peak occurring at a depth corresponding to a sputter time of 50 min. A probable zone of quasistoichiometric Pt_2Si is obtained sufficiently far from the top surface. A definite phase growth front corresponding to the oxygen peak position may be clearly identified in this profile. In the present experiment, oxygen is not introduced during the deposition step as it was the case in Refs. 22 and 31. This anomalous and partial Pt_2Si silicidation reaction is attributed to oxygen diffusion into the Pt film. Thus, two competitive diffusion process take place in opposite directions: oxygen present in the oven enclosure tends to diffuses into the Pt film while the Pt_2Si–Pt reaction front proceeds to the top surface. In a sufficiently thin Pt film (e.g., 15 nm), oxygen rapidly piles up at the Pt/Pt_2Si interface,[32] and acts as diffusion barrier for Pt. As a consequence, an annealing at 300 °C as long as 30 min is not sufficient to ensure the completion of the first Pt_2Si silicidation reaction. It is worth noting that experiments conducted in the RTA furnace (Secs. III C and III D) are not disturbed by oxygen penetration because samples are introduced at room temperature and also because a primary vacuum is realized before the introduction of the N_2/H_2 (97:3) gas flow and before activating the heating ramp.

F. Incomplete silicidation reaction due to a limited silicon source

The absence of a sufficient source of silicon atoms to complete the first Pt_2Si reaction is another possible cause for an abnormal termination of the silicidation mechanisms. In order to highlight this scenario, a 20 nm thick Pt film was evaporated on top of a very thin SOI layer and subsequently RTA annealed at 300 °C for 2 min. The full initial stack consists of the Pt overlayer, a 8 nm silicon SOI film, a buried oxide (BOX) of 400 nm, and finally the silicon back substrate. From Table I, the silicon thickness consumed by the Pt_2Si reaction is theoretically 13.2 nm. Therefore, this reaction is expected to terminate prematurely due to the default of one species (Si) in the active SOI film. Figure 12 perfectly illustrates this phenomenon through the XPS depth profile recorded across the Pt/Pt_2Si/SiO_2 stack after annealing. The original measurements of the Si $2p$ photoemission line has been fitted using a linear least squares algorithm in order to identify the chemical states of silicon. Excluding the 7 first minutes of sputtering characterized by an intermixed PtO layer, an unreacted Pt layer is clearly observed and characterized by a Pt $4f_{7/2}$ peak centered at 71 eV, indicative of a metallic state. A second zone where a silicidation reaction takes place is clearly identified in the 30–50 min sputtering interval. Over this region, chemical shifts of 1.5 and 0.6 eV are observed for the Pt $4f_{7/2}$ and Si $2p_{3/2}$ peak positions, as expected. Finally, the deeper part of the depth profile corresponds to the BOX region for which the peak positions of Si $2p_{3/2}$ (103.8 eV) and O $1s$ (533.1 eV) are consistent with the presence of oxide. In summary, special care must be taken for typical situations where thin SOI films, widely used in aggressive MOSFET architectures, are combined with a Pt silicidation step.[5–7] This discussion also consolidates the se-

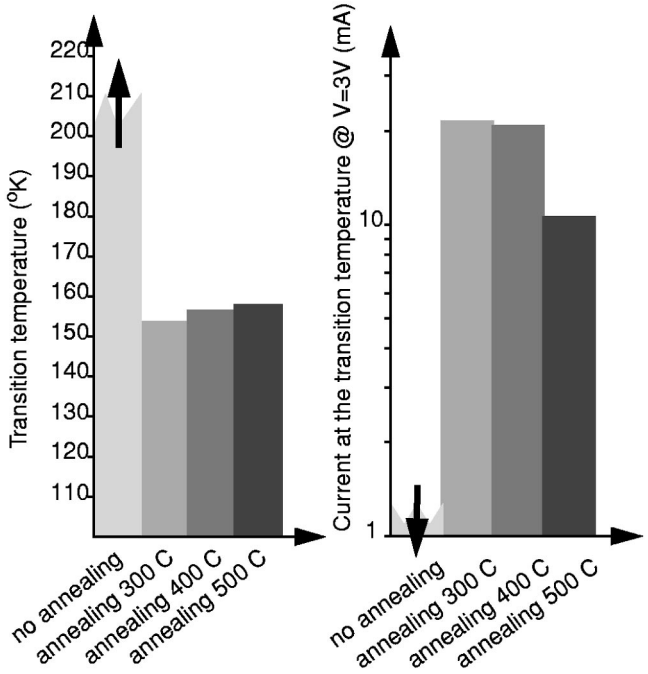

FIG. 13. Electrical characterization of Pt-based silicide contacts obtained at different temperatures (RTA treatment at 300, 400, and 500 °C). A low transition temperature and a high current drive are relevant of the best silicide obtained at 300 °C.

quential nature of Pt-based silicide reactions according to which the formation of the PtSi is possible only after the completion of the initial Pt_2Si transformation.

IV. ELECTRICAL MEASUREMENTS

Electrical measurements of Pt-based silicide contacts have been conducted to determine the annealing conditions that provide the lowest Schottky barrier to holes and, therefore, the lowest specific contact resistance that characterizes the carrier transport through the silicide/silicon interface. Both the transition temperature and the corresponding current level defined in Sec. II C have been extracted from current–voltage characteristics measured in the 170–300 K temperature range. This information is reported in Fig. 13 for different annealing conditions. First of all, the silicide contact formed at ambient temperature exhibits a very low current drive consistently associated to a very high transition temperature. This behavior is attributed to the noncontinuous and nonhomogeneous nature of the silicidation reaction deduced from the XPS depth profile in Fig. 6. The best electrical performance is obtained at an annealing temperature of 300 °C. For thermal treatments realized at higher temperature (400 and 500 °C), a slight decrease of the current drive is observed in conjunction with an increase of the transition temperature. This last performance degradation is attributed to silicon outdiffusion that forms a thin oxide layer with oxygen available at the top surface. This interpretation is corroborated by the corresponding XPS depth profiles of Figs. 9 and 10(a).

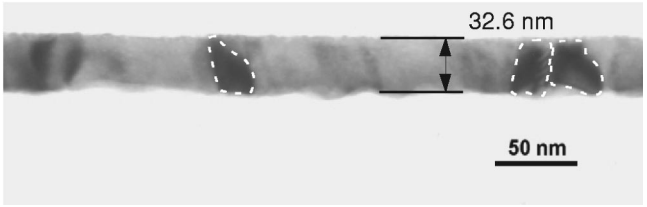

FIG. 14. TEM cross sections of a sample annealed at 300 °C by RTA for 2 min starting from a 15±1 nm Pt overlayer. A smooth and regular PtSi/Si interface is obtained. The thickness of the formed PtSi phase is in agreement with published expansion factors (see Table I).

V. TEM CROSS SECTIONS

TEM cross sections have been realized on a sample annealed by RTA at 300 °C starting from a 15±1 nm Pt overlayer. The corresponding images presented in Fig. 14 show a homogeneous PtSi film on which the vertical orientation of grains can be distinguished. No preferential site of growth can be observed and the silicide/silicon interface is smooth. The thickness ratio is $d_{Pt}/d_{PtSi} \sim 0.5$ which is consistent with the theoretical target given in Table I ($1/1.97=0.507$) and close to values found in the literature.[33]

VI. CONCLUSION

In summary, we have proposed a detailed study of Pt-based silicides obtained at room temperature, annealed in UHV or thermally activated by rapid thermal processing up to a temperature of 500 °C. XPS analysis was extensively used to characterize the kinetics and stochiometry of the Pt_2Si and PtSi phases. A remarkable agreement with kinetics parameters obtained by Stark *et al.*[12] has been obtained under UHV conditions. We have confirmed pileup of oxygen occurring at the Pt_2Si/Pt reaction front as an inhibiting factor of the silicidation. The incomplete silicidation of an ultrathin SOI film has been clearly outlined, providing on the same occasion a confirmation of the sequential nature of the disilicide/monosilicide reactions. Finally, current drive measurements on PtSi Schottky contacts have allowed us to identify 300 °C as an optimum annealing temperature.

[1] J. Chen, J. P. Colinge, D. Flandre, R. Gillon, J. P. Raskin, and D. Vanhoenacker, J. Electrochem. Soc. **144**, 2437 (1997).
[2] SIA Semiconductor Industry Association, "The International Technology Roadmap for Semiconductors—ITRS," 2001.
[3] S. Guha, E. Gusev, M. Copel, L. Ragnarson, and D. Buchanan, MRS Bull. **27**, 226 (2002).
[4] C. M. Osburn and K. R. Bellur, Thin Solid Films **332**, 428 (1998).
[5] J. R. Tucker, C. Wang, and P. S. Carney, Appl. Phys. Lett. **65**, 618 (1994).
[6] J. Kedzierski, P. Xuan, E. H. Anderson, J. Bokor, T. J. King, and C. Hu, Tech. Dig. - Int. Electron Devices Meet. , 57 (2000).
[7] E. Dubois and G. Larrieu, Solid-State Electron. **46**, 997 (2002).
[8] J. Derrien, in *Properties of Metal Silicides*, edited by K. Maex and M. Van Rossum (IEE INSPEC, 1995), p. 164.
[9] X. Zhenjia, in *Properties of Metal Silicides*, edited by K. Maex and M. Van Rossum (IEE INSPEC, 1995), p. 169.
[10] L. Ley, Y. Wang, V. Van Nguyen, S. Fisson, D. Souche, G. Vuye, and J. Rivory, Thin Solid Films **270**, 561 (1995).
[11] S. M. Zhou, M. Hundhausen, T. Shark, L. Y. Chen, and L. Ley, J. Vac. Sci. Technol. A **17**, 144 (1999).
[12] T. Stark, H. Grunleitner, M. Hundhausen, and L. Ley, Thin Solid Films **358**, 73 (2000).
[13] N. Franco, J. E. Klepeis, C. Bostedt, T. Van Buuren, C. Heske, O. Pankra-

tov, and L. J. Terminello, J. Electron Spectrosc. Relat. Phenom. **114–116**, 1191 (2001).
[14] *Multipak software manual*, *Physical electronics*, Vol. 50.
[15] S. Hofmann, in *Practical Surface Analysis*, 2nd ed., edited by D. Briggs and M. P. Seah (Wiley, New York, 1990).
[16] S. M. Sze, *Physics of Semiconductor Devices*, 2nd ed. (Wiley, New York, 1981).
[17] J. R. Jimenez, X. Xiao, J. C. Sturm, and P. W. Pellegreni, Appl. Phys. Lett. **67**, 506 (1995).
[18] C. R. Crowell and V. L. Rideout, Solid-State Electron. **12**, 89 (1969).
[19] F. A. Padovani and R. Stratton, Solid-State Electron. **9**, 695 (1966).
[20] F. A. Padovani and G. G. Sumner, J. Appl. Phys. **37**, 921 (1966).
[21] F. A. Padovani, Solid-State Electron. **11**, 193 (1968).
[22] C. A. Crider, J. M. Poate, J. E. Rowe, and T. T. Sheng, J. Appl. Phys. **52**, 2860 (1981).
[23] S. J. Morgan, R. H. Williams, and J. M. Mooney, Appl. Surf. Sci. **56–58**, 493 (1992).
[24] R. A. Donaton, S. Jin, H. Bender, T. Conard, I. Dewolf, K. Maex, A. Vantomme, and G. Langouche, Electrochem. Solid-State Lett. **2**, 195 (1999).
[25] J. C. Tsang, Y. Yokota, R. Matz, and G. Rubloff, Appl. Phys. Lett. **44**, 430 (1984).
[26] P. J. Grunthaner, F. J. Grunthaner, and A. Madhukar, J. Vac. Sci. Technol. **20**, 680 (1982).
[27] K. Hirose, I. Ohdomari, and M. Uda, Phys. Rev. B **37**, 6929 (1988).
[28] W. E. Morgan and J. R. Van Wazer, J. Phys. Chem. **77**, 96 (1973).
[29] J. W. Keister, J. E. Rowe, J. J. Kolodziej, and T. E. Madey, J. Vac. Sci. Technol. B **18**, 2174 (2000).
[30] M. L. Miller and R. W. Linton, Anal. Chem. **57**, 2314 (1985).
[31] J. B. Bindell, J. W. Colby, D. R. Wonsidler, J. M. Poate, D. K. Conley, and T. C. Tisone, Thin Solid Films **37**, 441 (1976).
[32] R. Schmiedl, V. Demuth, P. Lahnor, H. Godehardt, Y. Bodschwinna, C. Harder, H. P. Strunk, M. Schulz, and K. Heinz, Appl. Phys. A: Mater. Sci. Process. **62**, 223 (1996).
[33] S. P. Murarka, *Silicides for VLSI Applications* (Academic, New York, 1983).